High-precision bearing estimation for active sonar with cylindrical array, performed by interpolated array transformation

Wojciech LEŚNIAK

Gdansk University of Technology
Faculty of Electronics Telecommunications and Informatics
Narutowicza 11/12 80-233 Gdansk, Poland
wojciech.lesniak@eti.pg.gda.pl

The article presents a method for improving the accuracy of bearing in multibeam sonar with a cylindrical array. The antenna's non-linear shape and the resulting non-uniform sampling of the signal in space, mean that known methods of high-resolution spectral analysis cannot be used. In order to apply an algorithm from this group, a linear virtual antenna must be produced. The paper presents a technique of mapping a cylindrical array to the equivalent linear form. The simulation results present the accuracy of bearing estimation in the presence of white noise. Furthermore, the limitations of the method and practical aspects of the application in a real sonar system are discussed.

Keywords: interpolated array transformation

1. Introduction

Direction of arrival (DOA) estimation is one of the basic technical problems faced by radiolocation (RADAR) devices and, by analogy with the phenomena, underwater location systems (SONAR). Known for decades, the problem has been researched extensively producing a number of estimation methods. A broad overview of the methods is given in the paper [1]. Despite years of research, estimating the direction of arrival continues to be the topic of numerous studies. A lot of the work focuses on multi-element array systems, with the array's discrete elements uniformly spaced along a straight line. All known methods have been derived and described based on the model of a plane wave incident on a uniform linear array (ULA). Because the methods were originally developed for linear arrays, irregular arrays should be seen as a special case.

Estimating the direction of arrival goes hand-in-hand with the problem of estimating frequencies for discrete-time signals. There is a close relation between the frequency of acoustic pressure distribution sampled along a straight line, and the angle of incidence of the wavefront on that line. As a result, the accuracy of spatial frequency estimation determines the accuracy

of bearing estimation. As we know from the theory of signal processing, the higher the number of discrete samples, the greater the resolution of discrete frequencies of signal spectrum. The conclusion is simply that the more transducers an array has, the better the accuracy of determining the direction. While it is correct, this simple reasoning leads to impractical solutions. For obvious reasons, it is impossible to use an infinitely long antenna. In practice, antennas have finite dimensions. In the case of systems on board boats and ships, the basic constraint is the size of the vessel. Equipped with a linear antenna, underwater acoustic systems can in theory help to locate objects in the range of angles from $-90°$ to $+90°$ relative to the boresight of the array. In a multibeam system a lot of beams must be produced to cover the observation sector, making the range of listening limited to about $+/-40°$. This is the result of the increase in width of the deflected beam in a delay-sum beamformer [2]. Systems which require the full range of observation angles, use conformal arrays. In this case, hydroacoustic transducers are mounted on the shell plating. A full observation range can also be achieved by using the multi-element cylindrical array. In the classic multibeam sonar using a uniform cylindrical array (UCA), bearing accuracy is accepted as θ_{3dB} width of the receiving beam. Fig.(1) shows three neighbouring receiving beams generated in a delay-sum beamformer [3] for an $M = 36$ element array based on the signal received on neighbouring $N = 13$ transducers.

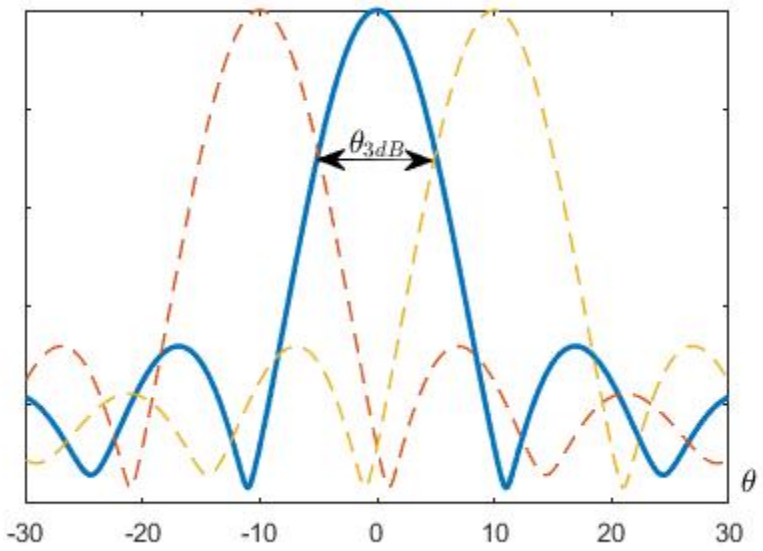

Fig. 1. Beam pattern of receiving beam based on $N = 13$ neighbouring transducers in a delay-sum beamformer for an $M = 36$ element cylindrical array.

The beam's width is the result of the cylinder's geometric dimensions, and is approximately equal to the angle between neighbouring transducer columns. This means that, in the case in question, the bearing of the object can be estimated with up to about $10°$ accuracy. Improving the accuracy of bearing would require additional columns with transducers mounted on the cylinder's surface. If the same relation between wavelength and the distance between neighbouring transducers is to be maintained, the diameter of the array must be increased. In some cases, this may prove impractical because of the array's physical dimensions, making the array too big to fit onto the ship's hull. If the cylinder can only take a limited number of array transducers, then, by analogy to arrays with a linear arrangement of transducers, the next best choice is to use known high-resolution methods [4]. There is a problem, however, when the methods are used directly with

a cylindrical array for bearing purposes. This is the result of array geometry which introduces non-uniform signal sampling in space. If achieved like this, the data is not good enough for spectrum estimation, due to errors, and cannot be relied upon. This can be solved by using a procedure to transform the shape of any array, including a cylindrical array, to a corresponding linear form. At present, there are two classes of transformation methods. These include Davies' transformation [5] and interpolated arrays such as Bronez [6], Friedlander [7] and Cook [8]. The result of interpolation is an array with uniformly spaced virtual hydrophones, which ensures the right conditions for signal sampling in space. This technique makes it possible to use high-resolution methods for bearing estimation in systems with a uniform cylindrical array.

2. Signal model

First, let us consider the model of a signal received by a multi-element uniform linear array. Let us assume that the echo is a narrow band signal and has this form

$$s(t) = p_k e^{j(2\pi f t + \varphi)} \tag{1}$$

where p_k is the amplitude of pressure, f is the signal frequency and φ is its initial phase. Let us also assume that echo source is located in the far field. Therefore, we can assume that the wave incident on the array is a locally plane wave. Fig.(2) shows the wavefront incident on the uniform linear array at angle θ_k.

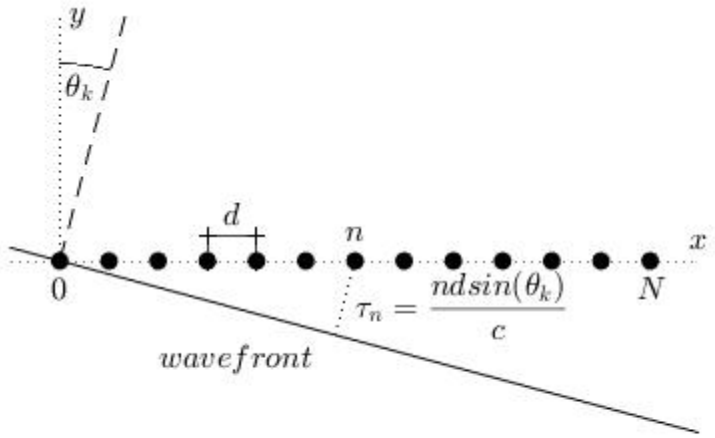

Fig. 2. Plane wave incident on a uniform linear array at angle θ_k.

The transducers are placed along the x line at equal d spaces between them. The time delay between the wavefront's equiphase surface and the successive transducers is expressed in the form

$$\tau_n = \frac{nd\sin(\theta_k)}{c} \tag{2}$$

where n is the number of array transducers, c is the velocity of acoustic wave propagation in a medium. For any moment of time the complex form of acoustic pressure measured at transducers placed along the array is expressed as follows

$$x_n(t) = p_k e^{j\left(2\pi \frac{c}{\lambda}(t+\tau_n)+\varphi\right)}, \qquad f = \frac{c}{\lambda} \tag{3}$$

where λ is the wavelength. Considering the fact that the array is built of a discrete number of N elements, the signal at the output of the individual transducers can be written as a vector

$$X(t) = \begin{bmatrix} x_1(t) \\ x_2(t) \\ \vdots \\ x_N(t) \end{bmatrix} = \begin{bmatrix} 1 \\ e^{j2\pi \frac{nd}{\lambda}\sin(\theta_k)} \\ \vdots \\ e^{j2\pi \frac{(N-1)d}{\lambda}\sin(\theta_k)} \end{bmatrix} p_k e^{j(2\pi f t+\varphi)} = a(\theta_k)s(t) \tag{4}$$

The column vector $a(\theta_k)$ steers the array and carries information about phase shifts of signal $s(t)$ received at transducer outputs. In addition, let us note that the form of the steering vector depends on the number and spatial distribution of the transducers, and on the angle of incidence of the wave. For a fixed moment of time t_0 the expression (4) takes this form

$$X(t_0) = \begin{bmatrix} 1 \\ e^{j2\pi \frac{nd}{\lambda}\sin(\theta_k)} \\ \vdots \\ e^{j2\pi \frac{(N-1)d}{\lambda}\sin(\theta_k)} \end{bmatrix} p_k e^{j(2\pi f t_0+\varphi)} = a(\theta_k)p_k e^{j\varphi_0} \tag{5}$$

and represents the distribution of acoustic pressure recorded by array elements along the straight line. As a result, the $a(\theta_k)$ steering vector describes a spatial signal along line x. By analogy to the signal in the time domain, if the expression nd/λ is treated as an equivalent of discrete time, then the expression $\sin(\theta_k)$ can be treated as an equivalent of frequency. Thus, the spatial distribution of pressure on array elements is a sinusoidal signal

$$a(\theta_k)^T = e^{j2\pi F_k n D}, \quad n = [0, \ldots, N-1], \quad D = \frac{d}{\lambda}, \quad F_k = \sin(\theta_k) \tag{6}$$

where F_k expressed the frequency of the spatial signal. As a result, estimating the direction of wave arrival is closely related to estimating the frequency of acoustic pressure distribution recorded at array transducers.

For the purposes of the simulation a cylindrical array model was used. It is made up of $M = 36$ columns spaced every 10° on the cylinder's surface. The cylinder's ray R was determined to ensure that the distance between neighbouring transducers would be half the wavelength $(d/\lambda = 0.5)$ of the sounding signal's centre frequency. The classic delay-sum beamformer generates receiving beams based on the signal received at neighbouring array elements. It was assumed that a single receiving beam is generated from $N = 13$ real array elements. The shape of the receiving beam is shown in Fig.(1). The neighbouring beams intersect at $-3dB$, and the range of angles between the intersections determines θ_{3dB} beamwidth. It is 10° and determines the system's bearing accuracy. To improve bearing accuracy within a single receiving beam, the Root-Music high-resolution frequency estimation method was chosen [10]. Fig.(3) shows a section of the array's cylinder with an active transducer section. With the transducers distributed as shown, signal sampling in the space domain becomes non-uniform. As a consequence, high-resolution methods for estimating the direction of wave arrival cannot be used

directly. Instead, a linear virtual array must be generated. As we can see, the virtual uniform linear array is placed along the chord which cuts across the extreme elements of the real array. Fact that the arc length is greater than the chord length, and keeping the spacing between the virtual transducers such as between the real ones, number of virtual elements K is reduced $(K < N)$.

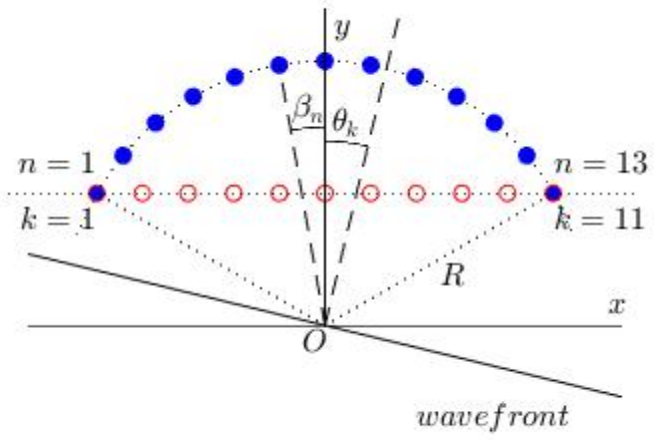

Fig. 3. Fragment of the cylindrical array and the corresponding linear virtual array.

Because of the geometry shown in Fig.(3) we can define the steering vectors for the real array

$$a(\theta_k) = \left[e^{jkRcos(\beta_1-\theta_k)}, \ldots, e^{jkRcos(\beta_N-\theta_k)}\right]^T, \quad k = \frac{2\pi}{\lambda} \tag{7}$$

and virtual array respectively.

$$b(\theta_k) = \left[e^{jk(x_1 sin(\theta_k)+y_1 cos(\theta_k))}, \ldots, e^{jk(x_K sin(\theta_k)+y_K cos(\theta_k))}\right]^T \tag{8}$$

Where x_k and y_k are the Cartesian coordinates of the position of virtual transducers. Vectors $a(\theta_k)$ and $b(\theta_k)$ describe the phase relations of the signal received at particular array elements. The vectors are determined relative to the joint point of reference, which is the wavefront going through the centre of cylinder O. By including the steering vectors, we can write the signal incident on the real transducers in this form

$$X(t) = a(\theta_k)s(t) \tag{9}$$

The signal received on the linear virtual array's transducers has this form

$$Y(t) = b(\theta_k)s(t) \tag{10}$$

3. Interpolated array transformation

The linear virtual array is the result of interpolation performed on samples of the signal received by real transducers (9). The transformation used in the simulation was proposed by

Friedlander [7]. It approximates the linear array in the least-squares sense for directions of arrival that fit within the optimisation sector defined as follows

$$\Delta\Theta = [\theta_1, \ldots, \theta_M] = [\theta_1, \theta_1 + \delta\theta, \ldots, \theta_M] \tag{11}$$

where θ_1 and θ_M are the left and the right boundaries of $\Delta\Theta$, $\delta\theta$ is the size of interpolation step. Using steering matrices A and B made up of steering vectors $a(\theta)$ (7) and $b(\theta)$ (8) determined for optimisation directions

$$A = [a(\theta_1), a(\theta_2), \ldots, a(\theta_M)] \tag{12}$$

$$B = [b(\theta_1), b(\theta_2), \ldots, b(\theta_M)] \tag{13}$$

a matrix of transformation T is built which solves the equation

$$T = \arg\min_T ||TA - B||_F^2 \tag{14}$$

where F denotes Frobenius norm [11]. In matrix notation the result of the equation (14) takes this form

$$T = BA^{\dagger} \tag{15}$$

where symbol $(\dagger)$ denotes the pseudo inverse matrix defined as follows

$$A^{\dagger} = A^H \left(AA^H\right)^{-1} \tag{16}$$

Considering this design of the transformation matrix T, signal Y at array virtual elements is determined as follows

$$TX(t) = T(a(\theta_k)s(t)) = \hat{b}(\theta_k)s(t) = \hat{Y}(t) \tag{17}$$

where $X(t)$ is the vector of input data recorded on the real array's transducers, $\hat{b}(\theta_k)$ is estimated steering vector of the virtual array. It is important to note that the transformation matches the steering vectors $a(\theta_k)$ to those of the virtual linear array in a least squares sense, for each angle within the sector of optimization.

Fig.(4) shows the normalised error of the transformation procedure defined as follows

$$e(\theta) = 20Log\frac{||Ta(\theta) - b(\theta)||}{K} \tag{18}$$

depending on the selected optimisation sector. The level of error is expressed in dB. Fig.(4) shows clearly that for wave arrival angles θ from the range outside the optimisation sector, the approximation error increases sharply in relation to the area inside the sector. We can also see the relation between the width of the selected range, and the accuracy of interpolation. The best results are achieved for a narrow 30° sector. For ranges of 60° and 90° respectively, while error levels clearly increase, they stay relatively low. For the broadest sector the error fits between -40 to -35 dB, which ensures a good array approximation in a broad range of wave arrival angles.

An important parameter that needs to be considered when designing the transformation matrix, is the matrix's condition number, defined with the formula

$$\kappa(T) = ||T|| \cdot ||T^{\dagger}|| \tag{19}$$

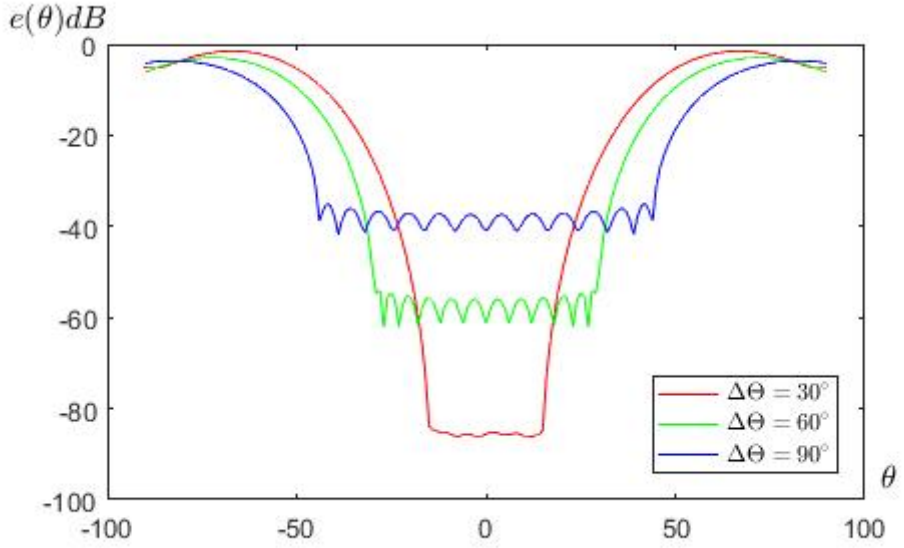

Fig. 4. Normalised transformation error depending on the selected optimisation sector versus angle of incidence θ.

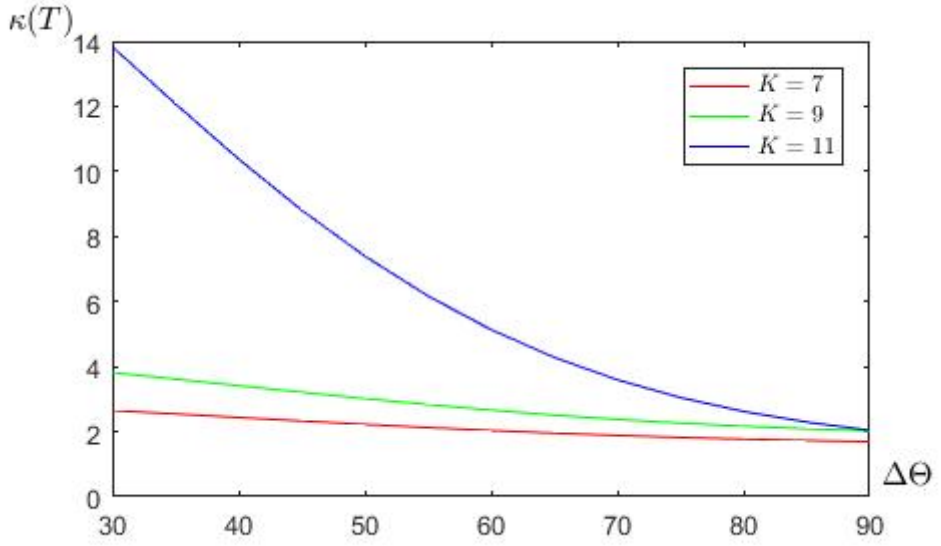

Fig. 5. Condition number of matrix T for a virtual array with $K = 7, 9, 11$ elements depending on the selected optimisation sector $\Delta\Theta$.

The parameter's numerical value defines how strongly the changes in input signal $X(t)$ affect the estimated signal $Y(t)$ in the linear system described with the relation (17). If the condition number is approximately equal to one, matrix T is well-conditioned, and defines the approximation procedure well. Fig.(5) shows how the selection of the optimisation sector and the number of interpolated virtual array transducers affects the value of the parameter. We can see clearly that for three different linear arrays with $K = 7, 9, 11$ elements, the condition number of matrix $\kappa(T)$ decreases as the width of the optimisation sector increases. In all three cases, the

value of the parameter is approaching a relatively low value, approximately equal to two. There are significant differences in the condition number in the narrowest sector of optimisation. It is clear from Fig.(4) and Fig.(5) that when designing the transformation matrix T, the width of the sector and number of estimated virtual transducers must be selected very carefully, due to their effect on approximation errors and their importance for how resistant the interpolation procedure will be to the noise that accompanies the input signal $X(t)$.

4. Simulation

Fig.(6) shows the block diagram of the simulated system. This is the receiving channel of the active sonar with a cylindrical array. Its sounding pulse is a signal with linear frequency modulation. The echo of the received signal is a shifted in time copy of the transmitting pulse, having this form

$$s_c(t) = e^{j\left(2\pi\left(f_o+\frac{B(t-\tau)}{2\tau}\right)t-\varphi_o\right)}, \quad 0 \leq t \leq \tau \tag{20}$$

The following signal parameters were considered: central frequency $f_o = 7,5kHz$, pulse duration $\tau = 800ms$ and bandwidth $B = 800Hz$.

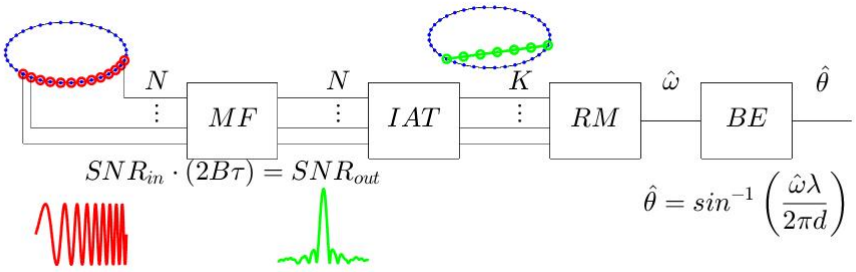

Fig. 6. Block diagram of the simulated system.

The echo signal is received by 36 columns spaced every 10° on the surface of the cylinder. The distance between the neighbouring array elements is half the wavelength of the signal's centre frequency. The echo signal in the presence of white noise is received on $N = 13$ active array elements indicated by the red circles. The received signal is sampled at sampling rate $F_s = 4f_o$, which is followed by matched filtering (MF block) to match the transmitting pulse. Filtration is performed in the frequency domain as follows

$$\phi_{SS}(t) = \mathscr{F}^{-1}(S_c(j\omega)^* X(j\omega)), \quad S_c(j\omega) = \mathscr{F}(s_c(t)), \quad X(j\omega) = \mathscr{F}(X(t)) \tag{21}$$

where $S_c^*(j\omega)$ is the conjugate spectrum of the transmitting chirp pulse, $X(j\omega)$ is the spectrum of the received echo and $\mathscr{F}$ and $\mathscr{F}^{-1}$ denotes the Fourier and inverse Fourier transform respectively. The result at matched filter output is a compressed echo signal with the following form

$$\phi_{SS}(t) = \phi_{SS_T}(t)e^{j2\pi f_o t} \approx sinc(\pi Bt)e^{j2\pi f_o t} \tag{22}$$

where ϕ_{SS_T} is the envelope of chirp (20) autocorrelation function, and as shown in [12], is very similar to a sinc function in the range of maximum. This is a narrow band signal with a frequency

equal to the centre frequency of the transmitting pulse. Because of the nature of the received signal, the problem of estimating the bearing of a broadband echo may be reduced to a much simpler case involving narrow band signals. Received echo is delayed by a time t_d, proportional to the distance between the transmitter and the target. Taking into account time delays due to the geometry of the antenna, as shown in Fig.(3) and expressed as

$$\tau_n = \frac{R\cos(\beta_n - \theta_k)}{c} \tag{23}$$

the output of the matched filter for N active transducers is as follows

$$\phi_{SSn}(t - t_d + \tau_n) \approx sinc(\pi B(t - t_d + \tau_n))e^{j2\pi f_o(t-t_d+\tau_n)} \tag{24}$$

Complex signal samples at N outputs of matched filters contain information about phase shifts in the particular receiving channels. Upon detection, a determination is made of the moment of time for which the matched filter output signal takes on maximum values. Taking maximum of sinc function as a value proportional to pressure p_k, the output of the filter can be expressed as

$$\phi_{SSn}(t - t_d + \tau_n) \approx e^{j2\pi f_o \tau_n} p_k e^{j2\pi f_o(t-t_d)} \approx a(\theta_k)s(t - t_d) \tag{25}$$

where $a(\theta_k)$ thing a steering vector (7). As can be seen, equation (25) takes the form of equation (9). The important is the phase difference between channels of the receiver expressed by steering vector (7). In addition, the effect of matched filtration is that the output signal to noise ratio SNR_{out} is clearly improved in relation to the input signal to noise ratio SNR_{in} on array transducers. The processing gain depends on the parameters of the sounding signal, and is expressed as follows

$$SNR_{out} = 2B\tau SNR_{in} \tag{26}$$

The presented results are for the output SNR_{out}, generally called the SNR further in the paper. For the set moment of time, a vector $X(t)$ of complex samples are collected, and due to the interpolation process a virtual linear antenna is formed. The vector $X(t)$ is multiplied by a previously defined transformation matrix T (IAT block). The end result is vector $\hat{Y}(t)$, which represents an equivalent of the signal received on a virtual linear transducer indicated by the green circles. Depending on the matrix, for a set optimisation sector, a linear array with $K = 7, 9, 11$ virtual transducers is estimated. The resultant vector $\hat{Y}(t)$ represents the spatial signal with frequency which depends on the angle of incidence of the wavefront on the virtual array θ_k. To estimate the spatial frequency the Root-Music algorithm was used (RM block), an extension of the basic direction estimator proposed by Schmidt [9]. Due to pulse compression, which is the result of matched filtration, it is assumed that echoes of different objects are clearly separated in the time domain. If that is the assumption, the Root-Music method searches for exactly one value of spatial pulsation $\hat{\omega}$. The bearing estimate (BE block) is related to spatial pulsation using this formula

$$\hat{\theta}_k = \sin^{-1}\left(\frac{\hat{\omega}\lambda}{2\pi d}\right) \tag{27}$$

In the simulation the worst case is considered, that is, estimating the bearing for maximum angle of incidence within θ_{3dB} beamwidth of a single receiver beam. For a 10° beamwidth, the maximum angle of wave front incidence relative to the axis of symmetry of the receiving beam is 5°. Because of the non-linear nature of relation (27), for this angle errors in spatial frequency estimation cause the biggest possible error in $\hat{\theta}_k$ angle estimation.

5. Results of the simulation

Fig.(7) shows the mean squared error of the estimated bearing defined as follows:

$$MSE(\theta) = \frac{1}{L}\sum_{l=1}^{L}(\theta_k - \hat{\theta}_k)^2 \tag{28}$$

where $L = 1000$ is number of tries and $\theta_k = 5^\circ$ is direction of arrival.

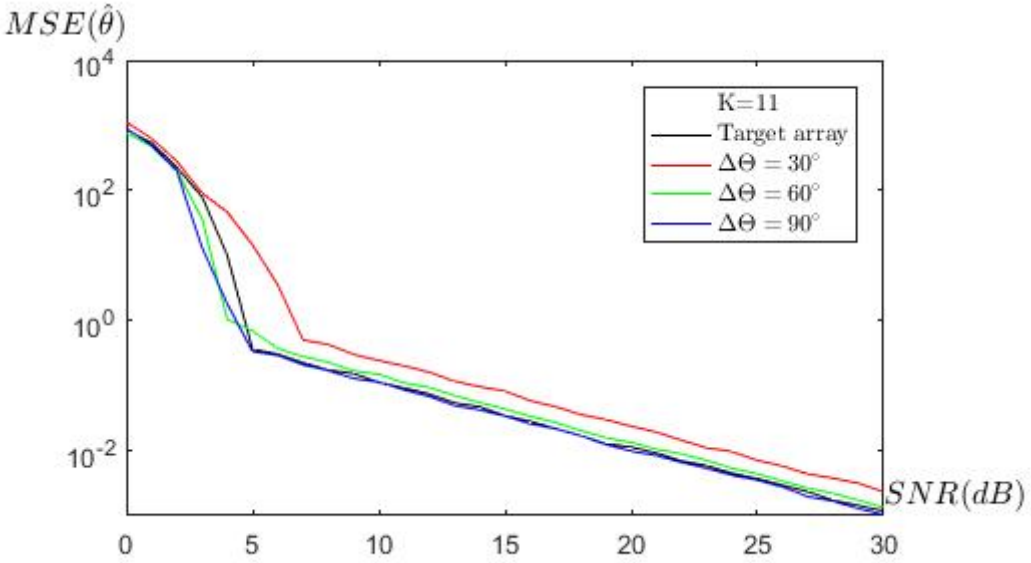

Fig. 7. Mean squared error for the antenna with K=11 elements optimised for three sectors $\Delta\Theta = 30^\circ, 60^\circ, 90^\circ$ and mean squared error for a real linear antenna.

For a virtual array built of $K = 11$ transducers and optimised for three different sectors $\Delta\Theta = 30^\circ, 60^\circ$ and 90° (red, green and blues lines respectively). In addition, Fig.(7) shows the mean squared error of bearing estimation for a real linear array, which is an array that is the desired result of interpolated transformation (black line). This is the target array, and one that is the point of reference when assessing bearing estimation errors. Fig.(7) shows that for a low level of SNR at matched filter output, the mean squared error is significantly large. It is important to remember, however, that underwater acoustic systems can detect signals if the signal-to-noise ratio is sufficiently high. This ensures a certain level of detection probability, and keeps the probability of a false alarm sufficiently low. For detection probability $P_d = 0.8$ and false alarm probability $P_{fa} = 10^{-5}$, the expected SNR at receiver output should be in the order of about 14 dB [13]. Given this SNR, the mean squared error of bearing is about 0.1°. Compared to the original 10° accuracy, bearing estimation has improved a hundredfold for a classic beamformer. An increasing SNR is accompanied by a more accurate bearing. Please note that the results obtained for approximation optimised in the sector $\Delta\Theta = 90^\circ$ are quite close to the results obtained for the real linear array (target array). Fig.(8) shows the results obtained for three arrays with $K = 7, 9$ and 11 elements, and optimised in the $\Delta\Theta = 90^\circ$ sector which has yielded the best results. It is clear in Fig.(8) that the mean squared error of bearing also depends on the number of approximated array elements.

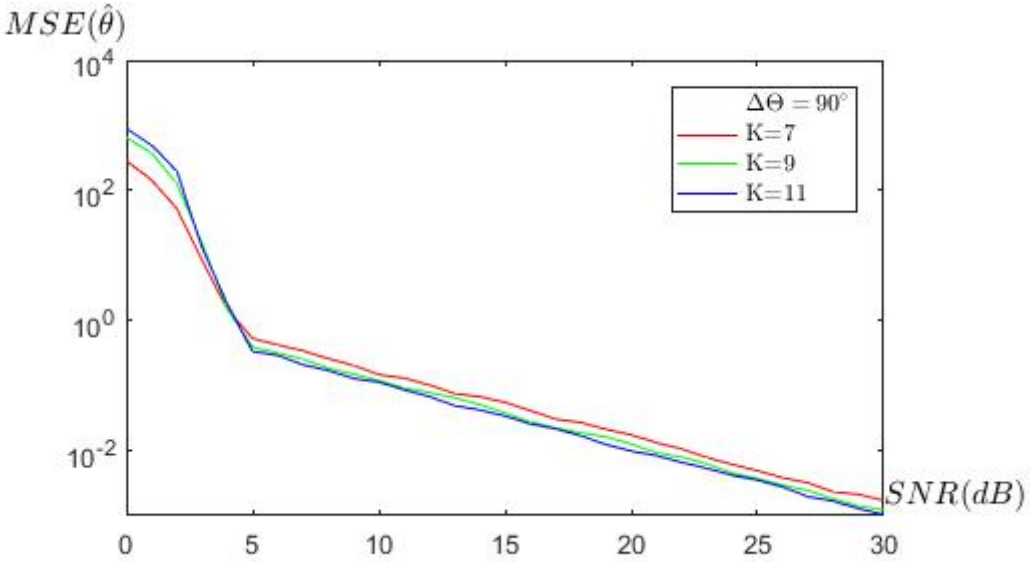

Fig. 8. Mean squared error for the antenna with $K = 7, 9, 11$ elements, optimised for the sector $\Delta\Theta = 90°$.

6. Conclusions

Interpolated array transformation helps to generate a linear virtual array using signal samples collected from non-linear array transducers. As a result, high-resolution methods can be used to estimate the direction of arrival in a sonar with cylindrical array. Simulation results have shown that bearing accuracy depends on the parameters of the transformation matrix T. Special attention should be paid to the matrix's condition number, whose value should be close to unity. It is important to note that the design and selection of the transformation matrix T, for a specific array, is done offline. The numerical cost of defining the matrix T is only incurred upon system design. The process of interpolation (17), which involves matrix multiplication, does not require any substantial computational effort. The results of the simulation have shown that a properly selected matrix T can create a virtual array, for which the method used for direction of arrival estimation gives results comparable to those obtained for the target linear array having the same dimensions. There is a significant hundredfold improvement of bearing accuracy in the simulated system, if the SNR at matched receiver output corresponds to the echo detection threshold. As well as improving the signal-to-noise ratio, matched filtration helps to compress the pulse of the received echo and, as a consequence, can separate in the time domain any echoes coming from other underwater objects. This keeps the problem of estimating the number of detected signal sources fairly simple, which is important for the Root-Music method. What is important, the method does not require any device modifications, and can be used in an existing sonar system. While the solution presented here should not replace the conventional delay-sum beamformer, it can be used as an additional tool for improving the accuracy of target bearing.

References

[1] H. Krim, M. Viberg, Two decades of array signal processing research: the parametric approach , IEEE Signal Processing Magazine (Volume:13 , Issue: 4) , pp. 64–97, Jul 1996.

[2] R. Salamon, Systemy hydrolokacyjne, ch. 9, pp. 547, 2006.

[3] J. Marszal, W. Leśniak, R. Salamon, A. Jedel, K. Zachariasz, PASSIVE SONAR-WITH CYLINDRICAL ARRAY, ARCHIVES OF ACOUSTICS Vol 31, No 4(S) , pp. 365–371, 2006.

[4] S. Lawrence Marple, Digital Spectral Analysis: With Applications, ch.6 - 13, January 1987.

[5] D. E. N. Davies, A transformation between the phasing techniques required for linear and circular aerial arrays, Electrical Engineers, Proceedings of the Institution of (Volume:112 , Issue: 11), pp. 2041 - 2045, November 1965.

[6] T. P. Bronez, Sector interpolation of non-uniform arrays for efficient high resolution bearing estimation, Acoustics, Speech, and Signal Processing, 1988. ICASSP-88., 1988 International Conference on, vol.5, pp. 2885 - 2888 , 11-14 Apr 1988.

[7] B. Friedlander, Direction finding using an interpolated array, Acoustics, Speech, and Signal Processing, 1990. ICASSP-90., 1990 International Conference on, vol.5, pp. 2951 -2954, 3-6 Apr 1990.

[8] G. J. Cook, B. K. Lau, Y. H. Leung, An alternative approach to interpolated array processing for uniform circular arrays, Circuits and Systems, 2002. APCCAS '02. 2002 Asia-Pacific Conference on (Volume:1) , pp. 411 - 414, 2002.

[9] R. Schmidt,Multiple emitter location and signal parameter estimation, IEEE Transactions on Antennas and Propagation (Volume:34 , Issue: 3), pp. 276 - 280, Mar 1986.

[10] H. K. Hwang, Zekeriya Aliyazicioglu, Marshall Grice, Anatoly Yakovlev, Direction of Ar-rival Estimation using a Root-MUSIC Algorithm, Proceedings of the International Multi-Conference of Engineers and Computer Scientists 2008, Vol II, 19-21 March 2008.

[11] P. E. Hyberg, Circular to linear array mapping using calibration data, HF Radio Systems and Techniques, 2000. Eighth International Conference on (IEE Conf. Publ. No. 474) , pp. 71 - 75, 2000.

[12] Achim Hein, Processing of SAR Data: Fundamentals, Signal Processing, Interferometry,ch.2, pp 38 - 44, 2004.

[13] R. Salamon, Systemy hydrolokacyjne, ch. 8, pp. 493, ch. 11, pp. 733-735, 2006.